Structural and Multidisciplinary Optimization manuscript No.
(will be inserted by the editor)

Bi-objective optimization of pylon-engine-nacelle assembly: weight vs. tip clearance criterion

Dimitri Bettebghor · Christophe Blondeau · David Toal · Hakki Eres

Received: date / Accepted: date

Abstract A realistic application of advanced structural and multi-objective optimization for the design of a fully assembled aircraft powerplant installation is presented. As opposed to the classical design process of powerplant installation that does not consider the influence of pylon sizing over engine efficiency, we develop in the present a fully integrated approach where both pylon and compressor intercase are designed at once. The main objective is to consider the impact of weight over tip clearance performance criterion and see how these two objectives are antagonistic. In this work, we perform in the same design session tasks traditionally devoted to the airframe manufacturer and aero-engine manufacturer. The overall weight of the assembly is minimized with respect to Specific Fuel Consumption (SFC) criterion. One interesting aspect of the process is that SFC criterion is based on highly proprietary models and its simulation and call within an optimization process is made available through the development of a webservice. One major phenomenon to consider in both pylon and engine design is Fan Blade Off (FBO) event, i.e. the sudden release of a blade. This event causes high impact loads and must be considered carefully in the design. Such a simulation is not an easy task and several nonlinear phenomena must be addressed (e.g. rotordynamics), not to mention the integration of this nonlinear dynamic response in a static structural optimization process. This article describes how the design of the full assembly is performed taking into account both objectives. Such a problem lies in multi-objective optimization field and then we describe the method we use to solve such a problem. The simulation of an FBO post-impact rotor dynamics is also described and we end up with the final results that show the influence of pylon-engine weight sizing over SFC.

Keywords Bi-objective optimization · Aircraft component design · Fan Blade Off simulation · Rotordynamics · Equivalent static load case · Thermo-mechanical model

D. Bettebghor
Onera, The French Aerospace Lab
Structural Dynamics and Aeroelasticity Department
Chatillon, France
Tel.: +33-(0)1-46734708
Fax: +33-(0)1-46734578
E-mail: dimitri.bettebghor@onera.fr

C. Blondeau
Onera, The French Aerospace Lab
Structural Dynamics and Aeroelasticity Department
Chatillon, France
Tel.: +33-(0)1-46734629
Fax: +33-(0)1-46734578
E-mail: christophe.blondeau@onera.fr

D. Toal
Computational Engineering & Design Research Group
University of Southampton
United Kingdom
Tel.: +44-2380597662
Fax: +44-2380594813
E-mail: djjt@soton.ac.uk

H. Eres
Computational Engineering & Design Research Group
University of Southampton
United Kingdom
Tel.: +44-2380598368
Fax: +44-2380594813
E-mail: Hakki.Eres@soton.ac.uk

1 Introduction

For wing-pod mounts aircraft, pylon and engine designs are highly correlated. Pylon designs depend, essentially, on critical loads. The pylon is designed to resist and

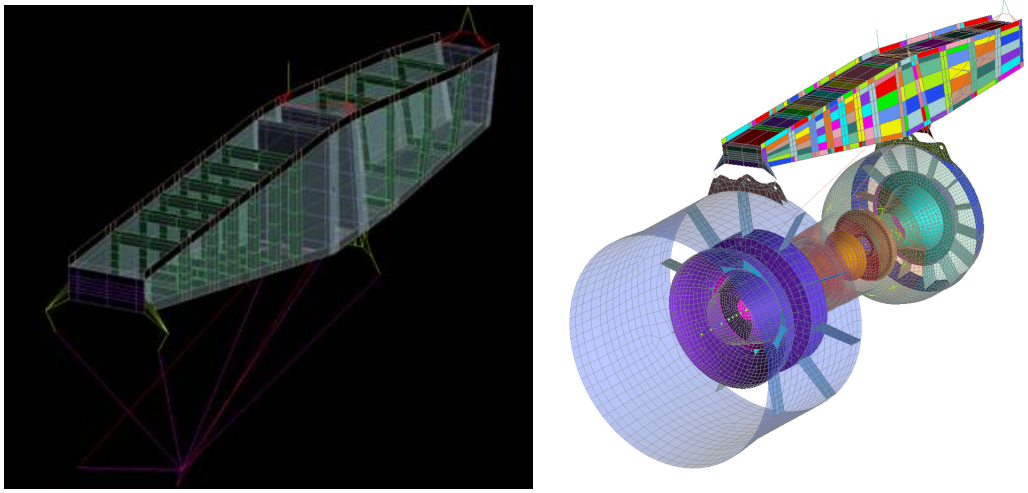

(a) Pylon model: transparency view (b) Assembly of pylon and engine

Fig. 1 (a) Pylon and (b) pylon-engine assembly.

redistribute loads for different regimes of the engine including thrust and maneuvers. A particular set of loads come from an highly critical event that is the FBO event. From a mechanical viewpoint, the pylon must be designed such that its bending and torsion stiffness are sufficiently high to resist the whole set of engine-generated loads. Engine design also highly depends on pylon design through loads redistribution. Additionally, engine mounts, as well as nacelle and nacelle struts must be designed for inertia loads coming from vertical and lateral maneuvers, thrust, gyroscopic effect, engine seizure [26]. Most of these loads depend on engine stiffness and also on pylon stiffness. From the point of view of efficiency, the engine must be designed in such a way that it attains minimum fuel consumption. A large proportion of fuel consumption comes from changes in the distance between the blade tips and the casing, see for instance [20]. The less this distance varies, the lower the fuel consumption. Roughly speaking, the engine design will seek to increase stiffness of the engine to reduce tip clearance. However, a heavy engine will increase loads in the pylon and hence increase the optimal weight of the pylon. The same way a very flexible pylon will increase loads within the engine. Common practice for the airframe manufacturer is then to perform pylon sizing with fixed engine-generated loads provided by the aero-engine manufacturer. It should be noted though that a first attempt to consider flexible loads, i.e. engine-generated loads that depend on pylon stiffness and then pylon sizing was considered in the framework of the European Research Project FP6 VIVACE [9].

Note that in this work, the flexible behavior of engine generated loads was not emphasized, but we rather focused on the antagonism between engine efficiency criterion and classical pylon sizing. Our main objective is to provide a realistic optimization process of engine installation taking into account several phenomena and criteria using middle-range fidelity numerical models. By 'middle-range fidelity models', we mean that we do not use a very detailed finite element model of the engine as the ones used by aero-engine manufacturers (with several millions degrees of freedom (DoF)) neither do we use a very simple model of the engine (as the ones typically used by airframe manufacturers) with several thousands DoF, as explained in [1] and [11]. Thanks to the context of this study, we have the opportunity to use not only a relatively sophisticated finite element model of the engine (several hundred thousands DoF) but also preliminary sizing models for pylon and nacelle. The two main criteria investigated are

- **Weight minimization** of pylon-engine-nacelle assembly.
- **SFC minimization** of the engine. As explained below, this is related to compressor tip clearance.

In this study, design variables include pylon panel thicknesses and intercase compressor thicknesses. As outlined before, FBO-loads are only used here to get a realistic design problem as these loads are often critical for sizing.

We first start by emphasizing the industrial and research context of the application. We describe the different models that we used to get to a whole assembly of pylon-engine-nacelle. The FBO simulation is briefly described together with the inherent issues with respect to the integration of a nonlinear transient mechanical response in a standard static linear structural design. Early results of the FBO analysis are presented. The en-

gine efficiency criterion used in this application, namely SFC of the engine is outlined. Details on its numerical simulation are also given. The numerical optimization algorithm used in this application for bi-objective optimization is described and some details about implementation are given. We finally depict the results we obtained that clearly show the influence of pylon sizing over engine efficiency criterion. More details on the models and preliminary modal analysis are shown in the appendices.

2 Description of the FEM models of pylon, engine, nacelle and interfaces

The models used in this work all come from aerospace industries. These models were exchanged within partners of the FP7 European Research Project CRESCENDO. We first briefly describe what the aim of this project was and then turn to the description of the submodels.

2.1 Context: CRESCENDO project

The project entitled '*Collaborative and Robust Engineering using Simulation Capability Enabling Next Design Optimisation*' (CRESCENDO) is an European Union co-funded R&T project with a budget of 55 M€, launched in May 2009. The project is led by Airbus and brings together 59 organizations from 13 different countries, including major aeronautics industry companies, service and IT solution providers, research centers and academic institutions. This project aims to make possible important step changes in modeling, simulation and virtualization. Above these overall objectives, CRESCENDO sub-projects for modeling and simulation target a reduction in the development life-cycle of 10%. This is where this study fits in, the objective of this application being to enable the airframe manufacturer to achieve faster a more mature designs by adding complexity at early design phases. This is the very innovative part of this application, since an engine efficiency criterion is integrated at preliminary design of the pylon.

2.2 Description of the FEM models and assembly

The pylon model was provided by Airbus, France. It consists in a typical pylon for a short range airliner and it is made of titanium. This pylon is depicted Fig. 1(a).

The pylon has several attachments to the wing and engine, these attachments are important since they will allow us to monitor the FBO loads for pylons:

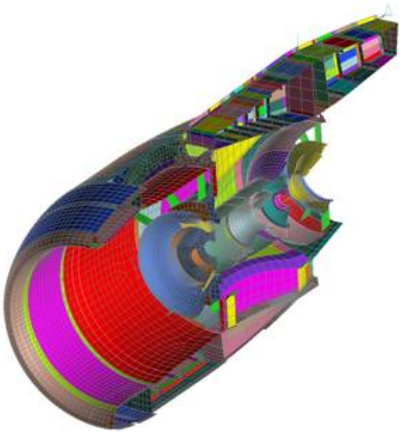

Fig. 2 Pylon-engine-nacelle assembly.

- For pylon-to-wing attachment, front attachment consists of two struts that only work under vertical loads. The rear attachment consists of a triangle under lateral and vertical loads. For axial loads (resulting from thrust and maneuvers), a strut known as a spigot is set in the middle of the upper skin to resist axial and lateral loads. We then have six DoF for the whole pylon-to-wing attachment as it is an isostatic junction.
- The engine-to-pylon attachment consists of 7 struts: 2 struts for the front mount attachment, 3 struts for the rear mount attachment and 2 thrust links. All of these struts are modeled as bars.

The engine model was provided by Rolls-Royce, UK and is presented in Fig. 1(b) while the nacelle model was provided by Bombardier Shorts, see Fig. 2. Note that the nacelle model features material nonlinearities since it has nonlinear friction elements (`CGAP`) for contact interface with sliding and friction (fan cowl/inlet, inlet/torque box, etc.).

The first task was to integrate and assemble the different sub-models to get a whole engine assembly. To do so the attachments between models need to be carefully defined. The scheme presented in Fig. 3 describes the layout of the engine to pylon attachments. On the engine side, the attachment links are modeled with a rod associated to a local coordinate system (`CD2`) aligned with the element axis (node `C`). On the engine side, a displacement interpolation element (`RBE3` type) has its master (dependent) node attached to a series of 6 unidirectional springs (3 translation and 3 rotation scalar stiffnesses). Additionally this node is associated to a local coordinate system (`CD1` at node `B`) different from `CD2`. The point here is to connect only the translational degrees of freedom of two coincident nodes associated to different displacement coordinate systems. This is done with a combination of an additional rigid ele-

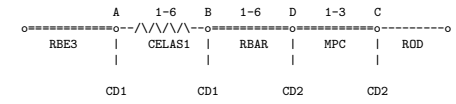

Fig. 3 Engine-to-pylon junction layout.

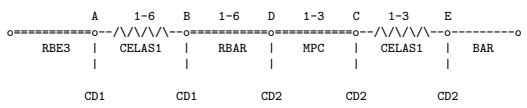

Fig. 4 Thrust-links-to-pylon junction layout.

ment (`RBAR`) to resolve the coordinate system mismatch and a multi-point constraint element (`MPC`) ensuring the translational displacement transfer.

The approach is similar for the thrust links-to-engine attachments except that three additional translational stiffnesses exist at the tip of the links, see Fig. 4.

3 FBO event numerical simulation

3.1 Generalities on FBO

A FBO event consists of a sudden release of a fan blade that may result from a typical high energy impact or fatigue. The level of the resulting force, this can be estimated through this simple formula,

$$F_{\text{unblc}} = m\omega^2 r. \tag{1}$$

For instance, let's assume a fan blade weight of 10 kg (realistic for aluminum/titanium blade), a nominal speed of 50 revolutions per second and a radius of 1 m, we get to $\omega = 50 \times 2\pi = 314.159\ \text{rad}\cdot\text{s}^{-1}$ and then,

$$F_{\text{unblc}} = 9.86.10^5\,\text{N}. \tag{2}$$

Such a force should be absorbed by the rotor without leading to a catastrophic failure of the rotor. To prevent such an issue, fuse elements are integrated at the bearing locations. Regarding the impact of the blade, the fan case should resist this high energy impact. A major milestone for engine certification is the FBO rig test where an actual engine is used. Regarding numerical simulation, the FBO event should be considered in the early design phase as the resulting loads are highly critical for both pylon and engine design. Numerical simulation of FBO is still a challenging and difficult task since many different nonlinear phenomena must be accurately predicted in order to achieve complete and realistic computations of associated loads. Over the past decade, the subject has raised considerable attention from both aircraft and engine manufacturers, see for instance [30], [21], [12], [22]. An excellent reference on FBO simulation from academia can be found in [14], where the author lists many different phenomena to be integrated in the simulation such as

- steady state pre-stresses in rotors,
- aerodynamic forces,
- failure criterion for metals,
- gyroscopic effects from spinning rotors attached to deformable cases,
- all possible interactions from the impact and contact of blades on casing (friction, rubbing, ...),
- many other nonlinear phenomena such as buckling, creep, elasto-plastic yielding, ...

A major challenge in this type of simulation is that there is no preferred numerical scheme for these nonlinear transient phenomena. Indeed, some of them may be more easily simulated with explicit schemes: contact, friction, ..., where a detailed three-dimensional elasticity model is needed while other are more likely to be simulated with implicit schemes: gyroscopic effects, ..., where a coarser model (with two-dimensional plate and shell elements) is sufficient. This would make the overall simulation of the whole FBO difficult to achieve with one specified type of numerical scheme. To overcome such difficulties, MD NASTRAN recently offered the capability to mix different levels of models and different numerical schemes for the same time simulation of FBO event [11].

At this point, it is worth noting that many of the aforementioned works are more the concern of the aero-engine manufacturer than that of the airframe manufacturer. Indeed for pylon sizing, the airframe manufacturer typically does not use the whole description of the pylon-engine-nacelle model and usually only has a coarse model of the engine. For early design phases, the airframe manufacturer assumes that the nacelle-engine assembly is rigid and only use FBO-loads transferred to the center of gravity of the engine. This way the airframe manufacturer does not take into account flexibility of the nacelle-engine assembly and its potential impact over FBO-loads. This assumption is still reasonable in the sense that it is mainly the loading in the engine-to-pylon attachment that drives the design process. Therefore, a coarse model of the engine or even a concentrated mass at the center of gravity of the engine is enough to perform pylon sizing with respect to the FBO event, provided that the airframe manufacturer has at disposal a correct set of FBO-loads.

3.2 Integration of FBO-loads into a static linear response structural optimization

A major issue in structural optimization is the integration of nonlinear dynamics responses within a given

optimization problem. Such responses might be used directly within constraints or as optimization loading cases. Whatever their use in the optimization problem, such responses are still challenging to integrate in a standard structural optimization problem for their transient and nonlinear characteristics. Note that this subject has raised considerable attention for many years, see for instance [13], [10], [3] and [32]. For such problems, the difficulty is twofold. First, sensitivity analysis of a nonlinear mechanics response might not be easy to achieve and second transient dynamics response can not be integrated as if in a structural optimization, since we can not easily define a continuous (then infinite) optimization constraint. FBO-loads based optimization combines both of these challenges. As stated in [6], mathematical theory for differentiability of nonlinear transient has not reached yet the level of maturity of other design sensitivity analyses (linear problems, geometric and material nonlinear problems). However, many different options to tackle such problems can be found in the literature: see for example [18], [16], [27], [5], [19]. Amongst them, one the most preferred options to treat nonlinearity is known as the *Equivalent Static Load Case* approach, which consists of deriving, from a nonlinear analysis, a static linear load case that gives either the same stress distribution or strain or even displacements. Regarding transient loads issues, one popular method is to reduce the time constraints into either a cumulative constraint over a time interval or constraints at given time steps. In any case, such time continuous constraints reduce to a finite number of static constraints.

In this application, we chose the simplest way to integrate FBO-loads within a static structural optimization by monitoring the engine-to-pylon and pylon-to-wing attachments. For each blade release angle, 0°, 90°, 180° and 270°, we identify time steps when each of the 11 DoF[1] of the attachment are minimum and maximum leading to 22 different time steps (see Fig. 5). For each time step, the load distribution for the engine case is stored as a load case. This process is done for each blade release angle leading to 88 static load cases.

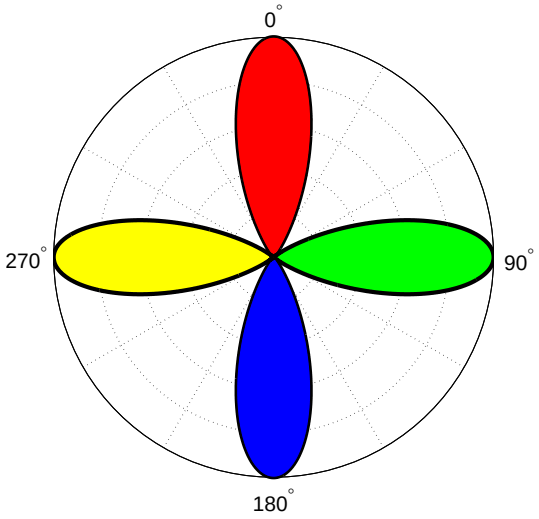

Fig. 5 Four blade release angles for the FBO simulation.

3.3 Practical implementation of FBO

As pointed out in [12], an essential ingredient of the FBO simulation is rotordynamics. Rotordynamics is the study of rotating machinery and structures. It is different from structural dynamics in the sense it also considers gyroscopic moments, cross-coupled forces and possibly whirling instability. However it is related to vibrations, since the main objectives of rotordynamics are to:

- **Predict critical speeds** for which vibrations due to rotor unbalance are at maximum to avoid them in operation.
- **Predict natural frequencies** of torsional vibration.
- **Predict dynamic instabilities**.

A rotordynamics simulation adds, to the classical equations of elastodynamics,

$$M\ddot{q}(t) + C\dot{q}(t) + Kq(t) = f(t), \tag{3}$$

additional effects due to centrifugal forces and rotating structures. These are added to the damping and the stiffness terms. The above equation then becomes,

$$M\ddot{q}(t) + (C+G)\dot{q}(t) + (K+N)q(t) = f(t), \tag{4}$$

where G is the gyroscopic damping matrix (proportional to rotor speed ω) and N the centrifugal forces. These matrices are not symmetric (G is skew-symmetric). These effects make the problem not symmetric any more. The eigenvalues of the system are then complex and specific strategies should be used (Campbell diagram, i.e. plot of complex natural frequencies versus rotation speed ω). A good introduction to vibrating and rotating machinery and structural dynamics can be found in [34] and [33].

One of the bottlenecks identified in the related literature on FBO is the issue of resonance. Indeed, in the case of a FBO event, the rotor speed slows down until it reaches the windmill speed. As it does so the rotor will pass through one of the fundamental frequencies of

[1] Thrust links can not be used to derive FBO-loads this way as their maximum loading is attained for normal engine regime.

the engine assembly resulting in large deformations as noted in [22], [21] and [4]. To ensure that we do not encounter such numerical issues a preliminary modal analysis was performed to identify the natural frequencies. The results of this preliminary modal analysis are described in Appendix A.

In this application, typical low pressure rotor speed ranges from 50 Hz to 10 Hz and high pressure rotor speed ranges from 120 Hz to 10 Hz. The natural eigenfrequencies of the assembly are depicted in Appendix A. It can be observed that there is no eigenfrequency within that range. For details about such resonance issues see [14].

As described in [11], a full FBO analysis requires three consecutive steps

1. **Pre-stress step:** Fan blade pre-stresses due to thrust, gravity and gyroscopic effects are computed. This step is typically performed over a detailed mesh with an implicit scheme.
2. **Fan blade off step:** The release of the blade is explicitly simulated together with damage of the blade, rubbing with the engine case, damage to the engine containment. The pre-stress state computed at Step 1 serves as initial condition of this step and this simulation is usually performed over a small time interval with small time steps.
3. **Post-impact loads step:** The forces calculated during Step 2 allow a transient analysis to be performed of the moments after the blade has impacted the casing. These forces are used as loads for a much longer analysis usually accomplished through an implicit scheme using a coarser mesh. This analysis covers the event until the engine run-down (rotor windmilling).

The first two steps are usually performed by the aero-engine manufacturer and usually involve proprietary data and models. These are computationally very expensive (especially Step 2 while Step 1 implies linear elasticity analysis , rotordynamics effects and possibly, depending on the geometry of the blade, geometric nonlinearities) since they are based on fine meshes (3D elements). The latter step is usually performed by the airframe manufacturer to get an estimate of FBO-loads for pylon sizing. The airframe manufacturer is given forces from Step 2 by the aero-engine manufacturer. These forces are

- **Blade impact loads on the engine case**.
- **Seizure** or **engine torque** due to rubbing loads.
- **Unbalance loads** coming from the mass of the missing blade material.

and to be complete, post-impact analysis needs the **fan rotor speed** as well. At this point, we should distinguish between the different analyses

- **Step 1 and 2** where most of the nonlinearity is predicted by the simulation. This is done by the aero-engine manufacturer and aims to insure that the engine containment will resist the high impact loads from blade off. In this analysis, rotor speed, unbalance and impact loads, seizure torque are only by-products at the engine level of the analysis. These two steps and particularly Step 2 remain challenging computational modeling tasks.
- **Step 3** where most of the nonlinearity is previously simulated (or gained from experiments, e.g. rotor speed) are transferred to the airframe manufacturer through '*engine level*' data, such as rotor speed, ... In this analysis, most of the nonlinearities are imposed as either boundary (or initial) conditions and occurs as forced functions on the right hand side.

Note that Step 3 is not an FBO simulation but a rotor dynamics simulation. It is essential for the airframe manufacturer but also for the aero-engine manufacturer since it provides a prediction of the performance of the engine after the event. In particular, when simulating the post-impact behavior, the aero-engine manufacturer will determine a windmill speed that may cause a high level of vibrations. However, in the related literature, these two different analyses are often treated separately, see [15], [30] for the first analysis and [12] for the second. In [11], the authors offer a solution to bridge the gap between the two types of analysis by mixing different models and numerical schemes while keeping proprietary information confidential.

In the present work, we only focused on Step 3, we then derived a set of FBO-loads compatible with the literature and ran a rotor dynamics simulation. These loads are depicted in Fig. 6. The event is simulated over one second and half to identify peaks in engine-to-pylon attachment responses. This transient simulation starts with a preliminary ramp-up of 0.1 s to properly set the initial conditions. We also have another 0.1 s of nominal rotor speed and thrust, which again sets the initial conditions before the FBO takes place. The FBO event then happens at $t = 0.2$ s and the rotor dynamics analysis is performed over a period of $1,5$ s to ensure that we reach the peak of each response.

At this point, the FBO induced loads for the rotor dynamics simulation are

- the **seizure torque** that is applied at the fan center location through a rigid body element connected to selected nodes of the fan case,
- the **thrust** that is applied to each thrust link,

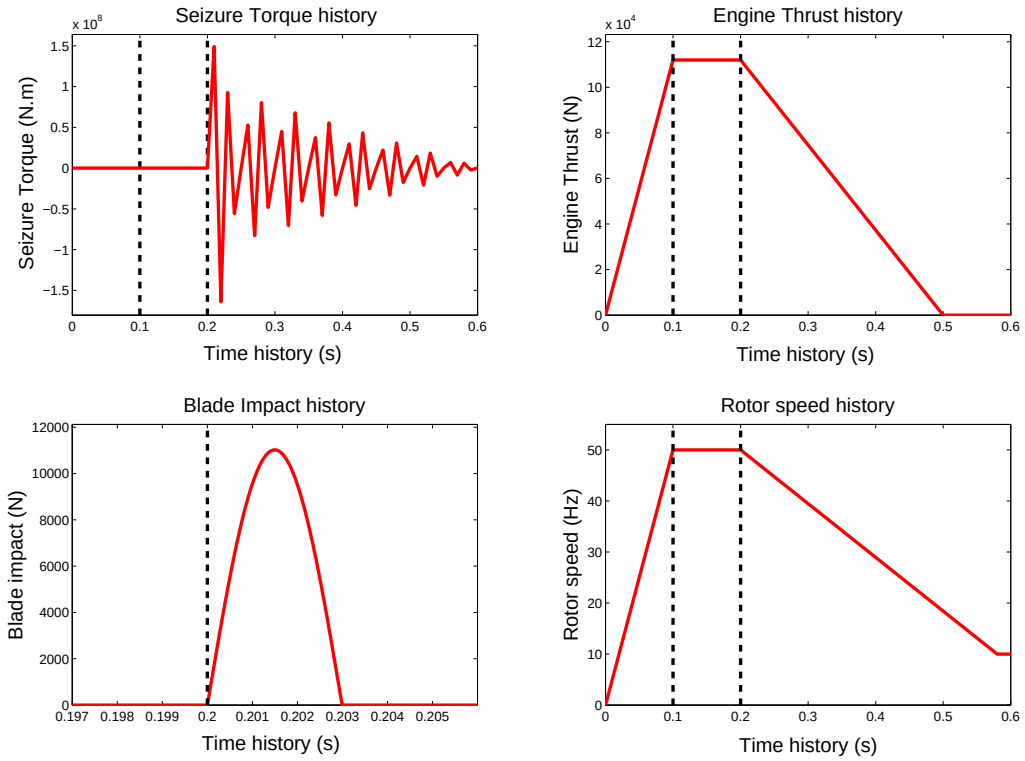

Fig. 6 FBO-loads for the rotor dynamics simulation.

– the **blade impact load** that is applied to the nodes of the engine case corresponding to the blade release angle.

Finally the gyroscopic effect and the unbalance load are applied using the Nastran `UNBALNC` and `RGYRO` cards. A rotor is specified through the `ROTORG` card and the rotor speed history in Fig. 6 is given as an input table. A structural damping of 8.5 % is imposed, based on relevant values found in the literature.

As specified earlier, we ran several simulations for different blade release angles. To retrieve forces at the fan case nodes, we used the `SPCFORCES` cards. Duration of this analysis is about 5 hours on a standard desktop computer.

4 Specific Fuel Consumption

This section further describes the engine efficiency criterion that we considered in this study. SFC (or more precisely in our case *Thrust Specific Fuel Consumption*) characterizes the engine's fuel efficiency. It is defined as the mass of fuel in grams (g) or pounds (lb) per unit time in second (s) or hour (h) per unit thrust in kilo-Newtons (kN) or pound-force (lbf). In our case, we will keep SI units, hence SFC will be defined as

$$[SFC] = \mathrm{g} \cdot \mathrm{s}^{-1} \cdot \mathrm{kN}^{-1}. \tag{5}$$

Typical values[2] of SFC for short-range aircraft (such as CFM-56 family for Airbus A320's) are in between $9\,\mathrm{g} \cdot \mathrm{s}^{-1} \cdot \mathrm{kN}^{-1}$ and $10.2\,\mathrm{g} \cdot \mathrm{s}^{-1} \cdot \mathrm{kN}^{-1}$ at take-off and in between $15\,\mathrm{g} \cdot \mathrm{s}^{-1} \cdot \mathrm{kN}^{-1}$ and $17\,\mathrm{g} \cdot \mathrm{s}^{-1} \cdot \mathrm{kN}^{-1}$ at cruise. From the related literature, it seems that SFC is by far lower at take-off, while the amount of thrust is at its highest level, than at cruise when the level of thrust is much lower.

A low SFC means high efficiency, therefore the objective is indeed to reduce SFC as much as possible. SFC depends on several factors, one of them being tip clearance, i.e. the gap between the blade tips and surrounding cases. As noted in [20], this clearance tends to vary with thermal and mechanical loads on the rotating and stationary structures. Furthermore, this clearance can change in an axisymmetric way due to uniform loading (thermal, internal pressure) and also in an asymmetric way due to non-uniform loads (thrust, maneuvers). As pointed out in [20], the control of tip clearance changes,

[2] See for instance `http://www.jet-engine.net/`

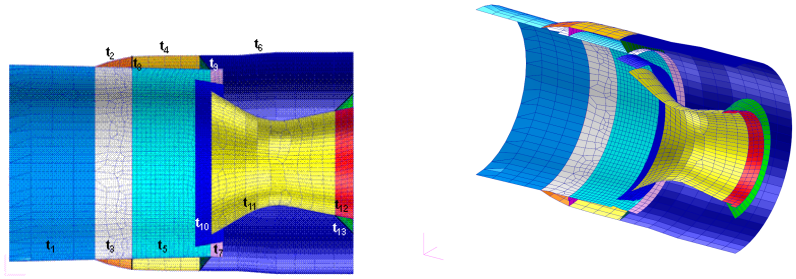

(a) (b)

Fig. 7 Parameterization of engine intercase compressor: design variables are wall thicknesses, tip clearance criterion is evaluated over these 13 variables.

especially in high pressure turbine (HPT) module, can provide a major reduction of SFC.

Generally, the stiffer the engine assembly the lower the SFC, meaning that in our CRESCENDO test case, the SFC will decrease as the thicknesses of intercase compressor panels increase as opposed to the weight of the pylon-engine assembly. Therefore, these two objectives are antagonistic. This antagonism should be considered carefully and more especially as flexibility is more and more important with high bypass ratio turbofan designs.

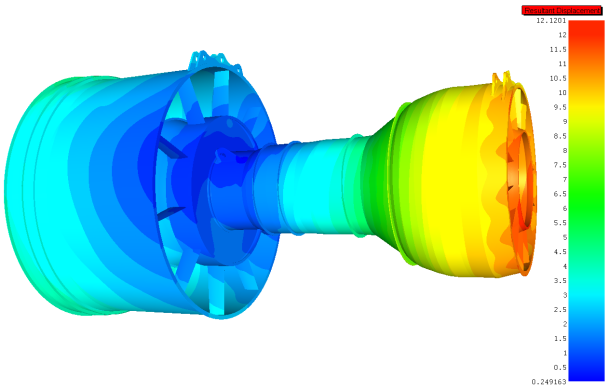

Fig. 8 Resultant displacements at cruise for the 3D casing.

4.1 Simulation of SFC based on a detailed mechanical model

As previously described an accurate indication of engine SFC can only be obtained with the use of proprietary models which the engine manufacturer may be reluctant to share with the airframe manufacturer. This restriction naturally hampers the ability to perform effective trade-offs between the engine design and that of the engine pylon assembly. Surrogate models offer a way around this problem by providing the airframe manufacturer with an accurate indication of the SFC of the engine with changing engine design parameters without the engine manufacturer providing access to proprietary tools. In order to enable the presented bi-level optimization a surrogate model of engine SFC with varying compressor intercasing thickness was constructed and hosted as a webservice.

The construction of this surrogate model involved a number of different software components all linked together within an Isight workflow. A 3D parametric CAD model employing the Siemens NX Open API was developed and used to modify the thickness of the compressor intercasing in 13 different locations. Given a set of thickness changes the parametrization generated a new model of the CRESCENDO test engine, which included the fan case, high and low pressure turbine cases and rear bearing housing as well as the new intercasing design. This tagged 3D model was then exported to the proprietary Rolls-Royce finite element solver SC03 where the geometry was meshed and the necessary boundary conditions applied.

The FE simulation of the static engine components consisted of an unstructured 10 node tetrahedral mesh with approximately 890 thousand elements. The boundary conditions are defined based on existing Rolls-Royce two shaft engines with pressures and temperatures defined over the whole engine. Although this model of the CRESCENDO engine is capable of performing a fully transient thermo-mechanical simulation, due to the large number of simulations required to construct the surrogate model and the cost of such transient simulations, the surrogate model is constructed using only mechanical simulations. Nevertheless, the simulation includes a number of design points during a typical engine cycle, take-off, cruise, gust and rotation loading conditions are all considered. While neglecting thermal effects reduces the accuracy of the tip clearance and therefore SFC prediction, the variation of SFC throughout the design space, when employing steady-state me-

chanical simulations, is closely correlated to that when employing transient thermo-mechanical simulations. For example, the two variable design space predicted by steady-state mechanical simulations for variations in thrust linkage setting angle and circumferential position is closely correlated to the design space predicted by transient thermo-mechanical simulations. In this case the design spaces have a r^2 correlation of 0.969 where,

$$r^2 = \left(\frac{\sum_{i=1}^{n}(x_i - \bar{x})(y_i - \bar{y})}{\sqrt{\sum_{i=1}^{n}(x_i - \bar{x})^2}\sqrt{\sum_{i=1}^{n}(y_i - \bar{y})^2}} \right)^2, \quad (6)$$

and a root mean square error (RMSE) of 0.25 where,

$$\text{RMSE} = \sqrt{\frac{1}{n}\sum_{i=1}^{n}(x_i - y_i)^2}, \quad (7)$$

with x and y denoting, in this case, SFC values resulting from mechanical and thermo-mechanical simulations respectively. $\bar{x}$ and $\bar{y}$ denote the mean SFC while n represents the number of sample points. In this case a total of 33 mechanical and thermo-mechanical simulations defined by an optimal Latin hypercube in two dimensions are used to calculate both the r^2 correlation and RMSE. The steady-state mechanical simulations employed here, therefore give an excellent indication of the overall trends in the design space but have minor errors in the precise values of SFC. These errors could be corrected by the utilization of a multi-fidelity surrogate modeling approach, such as Co-kriging[17], but this is beyond the scope of this paper.

Once the simulation has completed the displacement of the engine at 64 circumferential positions for each of the eight compressor stages and the front and rear bearings are extracted for the design points considered. An example of the displacements of an engine design at cruise are shown in Fig. 8.

The 3D mechanical simulation of the static engine components is complemented by a separate 2D simulation of the CRESCENDO engine rotor at the same design points. The displacements of each of the compressor stages are then combined with the displacements of the 3D casing simulation to determine the effective running clearance of the engine. First the 3D bearing displacements are used to determine the non-axisymmetric position of the rotor. The rotor tip positions are then used along with the casing displacements to calculate the circumferential closures for each stage of the compressor. The mean closure at cruise for each compressor stage is then subtracted from the pinch point closure for each stage and the root mean square value taken across all stages to give an effective running clearance for the compressor.

The effective running clearance for a new compressor design is then related to that of the baseline design and a change in compressor efficiency is calculated. It is assumed at this stage that a 1% change in effective running clearance directly translates into a 1% change in compressor efficiency. This new efficiency is then input into a PROOSIS performance model of the CRESCENDO engine and the SFC extracted.

Employing Isight and the proprietary Rolls-Royce optimization plug-in OPTIMATv2 an exhaustive design study of the 13 variable design space was undertaken and used to construct a surrogate model. A 400 point optimal max-min Latin hypercube sampling plan was first defined and a 3D mechanical simulation of the modified CRESCENDO engine carried out for each design. Approximately 80% of these simulations completed successfully with the remaining typically failing due to issues with the automated meshing process. The SFC resulting from each successful simulation was then used to create a Kriging model using the toolbox provided with OPTIMATv2 where the Kriging hyper-parameters are optimized using a hybridized particle swarm exploiting an adjoint of the likelihood function. More details on this process can be found in [31].

The accuracy of the resulting surrogate was then confirmed by carrying out a leave-one-out cross validation. During this process each of the sample points were removed in turn from the surrogate model dataset with the remaining data points, in conjunction with the optimized Kriging hyper-parameters, used to predict the SFC at the removed point. This produced a vector of predicted SFC values which could then be compared to the vector of actual SFC values, resulting from the mechanical simulations, to determine accuracy. In equations 6 and 7, x and y therefore become the vector of predicted and actual SFC values respectively. This process resulted in a RMSE of 5.36×10^{-2} and an r^2 correlation of 0.98 and therefore a surrogate model deemed to be of sufficient accuracy for optimization without the evaluation of any additional update points. At this point it should be reiterated that it is assumed, based on the results for the simpler two variable design space, that the surrogate model of SFC constructed using mechanical simulations will follow the general trend of the thermo-mechanical design space. In theory the accuracy of this model could be improved by including a small number of thermo-mechanical simulations within the dataset in the form of a Co-kriging model but, once again, this is beyond the scope of this paper.

Given a constructed model OPTIMATv2 is capable of then generating an Excel file with this surrogate model embedded within it. This Excel file can be protected and given directly to partner organizations or, as is the case here, used to deploy a webservice.

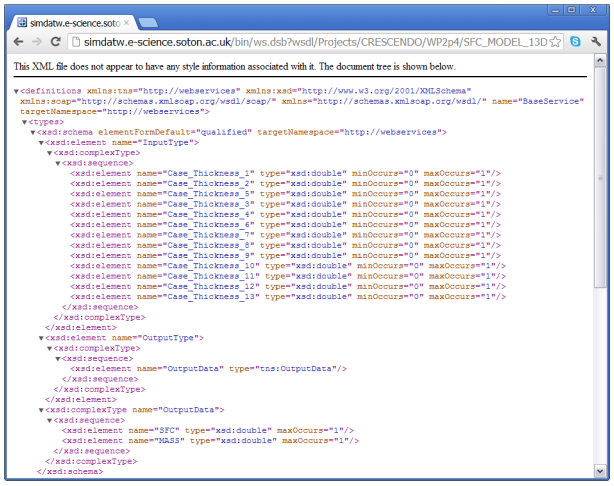

Fig. 9 WSDL details of the surrogate model running as a webservice.

4.2 External access for SFC through webservices

The most pragmatic way of converting the surrogate model in Excel into a webservice is to use Vanguard Studio. This tool can access and run any Excel spreadsheet as a component as long as the spreadsheet has named input and output cells. To this end, OPTIMATv2 generated surrogate model is further processed to define all input and output cells by utilizing Excel's 'Create from Selection' functionality in the 'Formulas Defined Names' ribbon. After embedding the surrogate model into Vanguard Studio, this new surrogate model is then published on the Vanguard server that automatically generates the Webservice Definition Language (WSDL) interface of the surrogate model (see Fig. 9).

This webservice can easily be accessed programmatically by using Java, MATLAB, Microsoft Visual Studio, or any other platform that supports the webservices standards. Encapsulating the simulation results in an Excel surrogate model and then converting this model into a webservice adds another layer of security and converts the whole optimization process into a black-box. Hence, it enables collaboration between industrial partners within the extended enterprise while protecting individual partner's intellectual properties.

5 Implementation details and results

5.1 Design variables and optimization constraints

As stated earlier, the set of design variables addresses both pylon and engine intercase compressor. More precisely, 80 design variables parameterize the pylon panels, they are panels and spar thicknesses defined through constant thickness regions. More precisely there are four different types of such variables

- Spar flanges,
- Spar webs,
- Panel flanges,
- Panel webs.

The minimum thickness value is fixed to 2 mm. Another 13 design variables parameterize the compressor intercase, they are as well panels thicknesses. Real design variables are variation of thicknesses with respect to their nominal value. These parameterizations are depicted in Figs. 7 and 10. This set of variables are denoted as x.

The objective functions are the weight of the overall assembly, $W(x)$ and the surrogate model of SFC, $S\hat{F}C(x)$. Sensitivities of these objective functions are easily derived. Optimization constraints are the following:

- **Pylon constraints:** For pylon sizing, stress in panels and spars are constrained. Major principal stress distribution $\sigma_{\max}$ is constrained to be lower than titanium's yield tensile stress. Minor principal stress distribution $\sigma_{\min}$ is constrained to be greater than titanium's yield compressive stress. Maximum shear strain $(\sigma_{\max} - \sigma_{\min})/2$ is also constrained.
- **Compressor intercase constraints:** A variation of 10% around the nominal value of the Von Mises stress distribution is imposed.

Regarding critical load cases, as mentioned earlier, FBO-loads translate into 88 static load cases. Another 21 load cases, supplied by Airbus, France are equivalent static load case for fatigue. Results of the Von Mises stress for all 88 FBO equivalent static load cases are depicted in Fig. 11.

5.2 Multi-objective optimization

This type of optimization problem falls in the multi-objective optimization field. A quite rigorous and general introduction can be found in [25]. The major idea is to find out not only one optimal design but a front of optimal design points that are all optimal in an multi-objective way. This optimality is known as Pareto optimality and a design point is said to be Pareto-optimal whenever any improvement of one objective degrades one of the other objectives. The set of all Pareto-optimal points is the Pareto front. Our main goal is then to provide for our CRESCENDO test case the Pareto front of pylon-engine assembly weight vs. engine SFC. To do

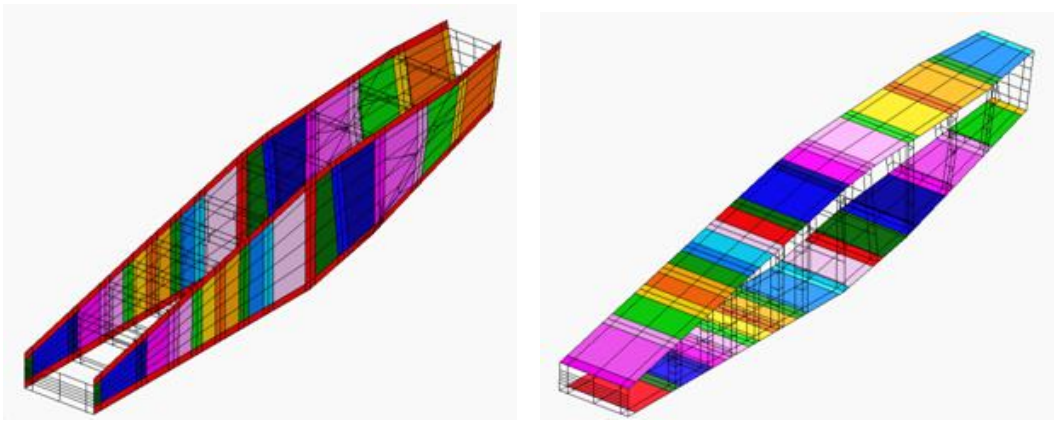

(a) (b)

Fig. 10 Parameterization of pylon: the 80 design variables are wall thicknesses.

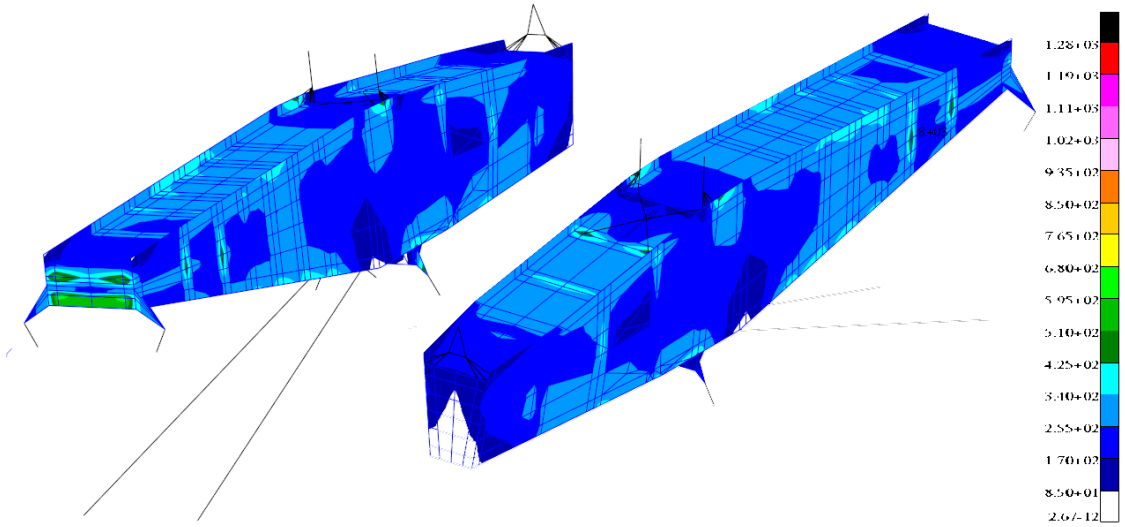

Fig. 11 Von Mises stress distribution for equivalent static load cases from FBO rotordynamics simulation. The Von Mises stress is taken as the maximum over the pylon for all 88 static load cases derived from nonlinear transient simulation. Pylon front view (left) Pylon rear view (right).

so, we assembled a composite function parameterized by a weight factor $\alpha \in [0, 1]$,

$$F_\alpha(x) = \alpha W(x) + (1 - \alpha) S\hat{F}C(x) \tag{8}$$

Then F_α is minimized with respect to x. As usual in such scalar method, the real functions are not considered rather than their following normalization transformations

$$W_{\text{norm}}(x) = \frac{W(x) - W_{\min}}{W_{\max} - W_{\min}} \tag{9}$$

where $W_{\max}$ and $W_{\min}$ refer to the maximum and minimum values of W without taking into account the other objective namely $S\hat{F}C$. It is obtained by standard mono-objective optimization of function W. Only structural constraints are taken into account while performing this optimization. In our case, it simply consists in computing the weight value for the maximum thickness. The same goes for $S\hat{F}C$, however computation of $S\hat{F}C_{max}$ (and $S\hat{F}C_{min}$) relied on a real mono-objective optimization[3]. There exist many different normalization transformation of objectives. The normalization in Eq. 9 used here is described in [28] and is often reported as the most robust normalization [23]. Practically, the minimization of F_α is performed with MSC.Nastran SOL200, the composite function F_α is computed and integrated in the SOL200 session with the help of the external response for a user-supplied subroutine (`DRESP3` card). The overall session is parameterized and the $[0, 1]$ line is spanned. For each value of α_i, one optimization is performed and the optimal associated design $x_i^\star$ is re-

[3] $(W_{\min}, SFC_{\min})$ is known as the *utopia point* (usually not reachable) and $(W_{\max}, SFC_{\max})$ is known as the *nadir point*.

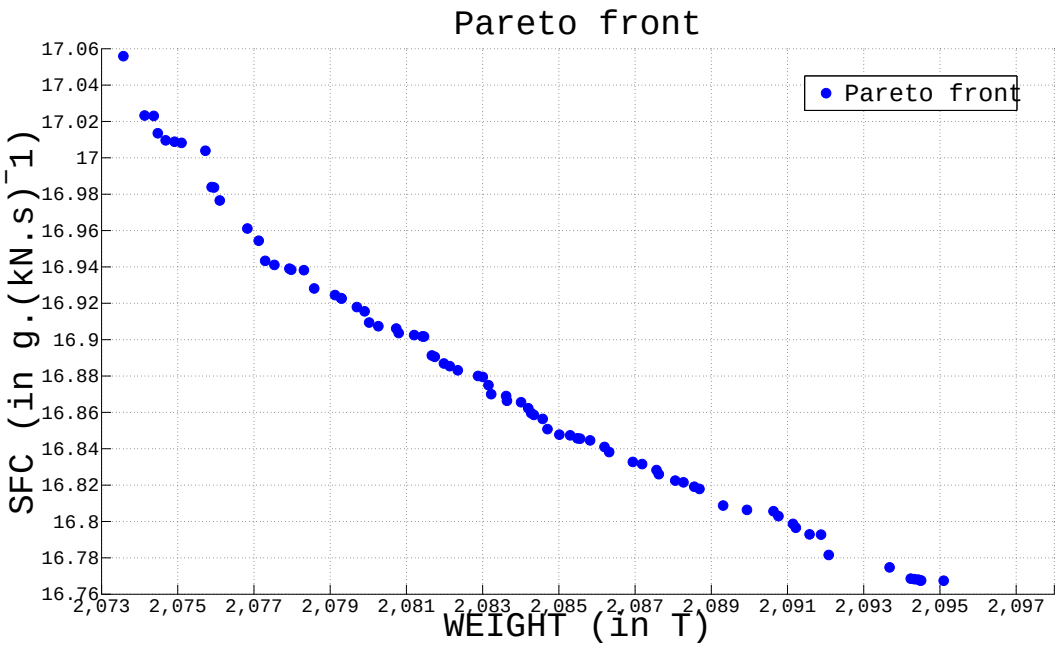

Fig. 12 Final Pareto front obtained with 80 scalar optimizations with MSC Nastran SOL200

tained whenever termination criteria are satisfied, leading to a point $(W(x_i^\star), S\hat{F}C(x_i^\star))$. After N scalar optimizations, the set of all points $(W(x_i^\star), S\hat{F}C(x_i^\star)_{i=1\ldots N})$ is post-processed to get Pareto-optimal points. This method is the *Weighted Sum Method* and it is one of the most popular method for multi-objective optimization. However as noted in the survey article [23], it has some important drawbacks. The most important one is that only convex parts of the Pareto front can be obtained from this method. Next the choice of a set of good weighting coefficients α_i can be quite challenging. In our case, we chose a strategy described in [29] known as the *eigenvalue method*. About 200 scalar optimizations were performed and the average duration for one scalar optimization was 4 hours. From these 200 scalar optimization, a final set of 80 optimal designs was sorted.

5.3 Final Pareto front

The final Pareto front that we obtained is depicted in Fig. 12. We observe that we almost span uniformly the utopia line, that is the line between the two individual optimums, which would indicate that we do not miss large parts of the real Pareto front. From numerical tests (signature of approximated Hessian matrices for uniformly distributed points in the design space), both objectives functions appear to be convex over design variables. The fact that some scalar optimizations (120) did not converge to a Pareto-optimal solution does not necessarily infer the convexity of objectives functions. Indeed, some convergence issues and numerical inaccuracies can also explain why for some values of the weighting coefficient α, the objectives at convergence are not Pareto optimal but they are, however, quite close to the front.

We observe that a decrease in weight of 22 kg increases SFC by about 0.3 g·(kN·s)$^{-1}$. This amount of SFC represents for instance for a standard engine for Airbus A320 of 120 kN of thrust for a one-hour flight more than 150 liters of fuel. From this final Pareto front, we observe that engine (or at least compressor intercase) flexibility has a quite negative impact on overall aircraft performance. This indicates that the flexibility of the engine must be considered to efficiently predict and validate SFC. From the airframe manufacturers point of view, such a front of potential pylon-engine designs is useful to select a pylon design by evaluating its impact over engine performance.

6 Conclusion and future work

We presented an original industrial application of classical and advanced tools from structural and multidisciplinary optimization for an aircraft powerplant installation. The main innovation is that both classical weight performance and tip clearance criterion are considered jointly in the same optimization problem. To consider both objectives, a classical multi-objective strategy was used. As in an industrial design process, loads from

FBO should be considered for pylon sizing, a preliminary nonlinear rotor dynamics simulation was performed to derive through an equivalent static load case approach a set of critical load cases to be integrated in the structural optimization problem. The tip clearance criterion simulation was performed through detailed and proprietary engine mechanical models that are parameterized by the same engine design variables. The results of this simulation were made available through a remote application. The objective function was then integrated in the design session as an external user subroutine (`DRESP3` card in Nastran). Final results led to a Pareto front where the influence of pylon sizing over engine efficiency can be appreciated. This Pareto front can help both airframe and aero-engine manufacturers make decision and trade-offs between overall weight and efficiency.

Regarding potential improvements, this bi-criteria design could benefit from several enhancements to reach maturity. Amongst them, the most significant is to consider FBO-loads as flexible, i.e. design variables dependent. Indeed, while tailoring pylon stiffness to reach desired performance, the FBO equivalent load cases change since the redistribution of loads changes. This means that at each iteration of the optimization, the FBO load cases change. To take into account these flexible loads, one should call the nonlinear rotor dynamics analysis and derive equivalent static load case by post-processing the simulation results at each change of design variables. To be even more efficient and to converge faster, one could derive sensitivities of stress and strain distribution resulting from equivalent load case with respect to design variables. Call L_{FBO} the equivalent load case for a given value $x^\star$ of design variables. These forces and moments do depend on $x^\star$. Call d_{FBO} the resulting displacement distribution that satisfy

$$K(x^\star)d_{\text{FBO}}(x^\star) = L_{\text{FBO}}(x^\star) \tag{10}$$

with K the stiffness matrix. To get the sensitivity for displacements constraints (or stress and strain distributions), one would need

$$\frac{\partial d_{\text{FBO}}}{\partial x_i} = -K^{-1}\Big(\frac{\partial K}{\partial x_i} - \frac{\partial L_{\text{FBO}}}{\partial x_i}\Big) \tag{11}$$

where the $\partial L_{\text{FBO}}/\partial x_i$ term is of course quite challenging to obtain apart from a finite difference approach which can be too costly. It is a typical situation where surrogate models could help. Indeed, mechanical responses for post-FBO rotordynamics simulation and then L_{FBO} the equivalent load case could be computed off-line for a sample $(x^{(i)})_{i=1\ldots N}$ of design variables (in the case of pylon thicknesses, the sample $(x^{(i)})_{i=1\ldots N}$ then refers to N potential designs of the pylon) and one can construct response surfaces of the mechanical responses or the function $L_{\text{FBO}}(.)$ or even better of $d_{\text{FBO}}(.)$. This way the difficult term $\partial L_{\text{FBO}}/\partial x_i$ could be approximated by the derivative of the response surface model. The existing finite element model of pylon could of course be used to build response surfaces. However, in practice doing so we would face a major difficulty which is the dimension of the input space. Indeed, if we take the existing pylon model, the input space of the response surface would be all the pylon design variables (about one hundred). Construction of response surfaces for such dimensions is very unlikely to be accurate, for often reported limit for dimension of response surface construction (whenever it is kriging, neural nets, radial basis functions, support vector regressions) is about 15-20 (see for kriging for instance [7]). There are of course surrogate models better suited for high dimensional problems (such as Multivariate Adaptive Regressive Splines, tree-based methods), however they often exhibit a poor accuracy. Regarding this subject of dimensionality, a comparison of existing methods (with the notable exception of Gaussian Process a.k.a kriging) can be found in [8]. To cope with this celebrated problem known as '*the curse of dimensionality*' an alternative approach would be to derive first an equivalent beam model of the pylon (or multi-beam to be more realistic) and build a response surface model post-FBO responses of load cases from beam characteristics $EI(x^\star)$, $GJ(x^\star)$, ... to $L_{\text{FBO}}(x^\star)$. This would yield a considerable number of response surface models to build, but each of them would be of reasonable input dimension. Part of the difficulty for such an approach would be first to assess its correctness and demonstrate that a complex structure such as a pylon can be reduced to a multi-beam model. This could be done with a global sensitivity analysis that would give the dependence of post-FBO nonlinear rotordynamics results with respect to detailed design variables (wall thickness') as opposed to the same dependence with respect to multi-beam mechanical characteristics. In case such a reduction is validated another difficulty would be to build a correct design of experiments over equivalent beam-model characteristics, as a uniform design of experiments over detailed design variables needs not be transported into a uniform design of experiments over multi-beam model mechanical characteristics.

Another valuable benefit would be to add more disciplines to the design. In particular, thermal effects are quite important to consider for pylon and pylon fairing design and also for their thermoelastic effects: temperature dependent material, creep or thermal buckling phenomena. Similarly the proprietary steady-state mechanical simulations of the engine tip clearances could

be replaced by high fidelity transient thermo-mechanical simulations which would give a more accurate prediction of SFC and provide thermal loads to the pylon and pylon fairing analysis. A multi-fidelity surrogate modeling approach could be utilized to create the response surfaces for collaboration thereby reducing the number of expensive thermo-mechanical simulations required.

Such an integrated analysis and design would potentially help identify more mature design at earlier development phases. Finally the innovative industrial application presented here can be thought as the structural design process of a more conceptual level where position of the pylon over the wing would be optimized not only with respect to the structural design but also with respect to the aerodynamic design. Such a conceptual design phase will be treated in a future work.

Part of this present work was to demonstrate the capability to merge in the same optimization and design several disciplines including proprietary and confidential data through the use of surrogate models. To achieve a realistic design, FBO rotor dynamics simulation was necessary. In this work both FBO-loads and tip clearance criterion in pylon structural optimization were integrated with the help of different numerical capabilities and expertises.

Acknowledgements The research leading to the presented results received funding from the European Community Seventh Framework Programme (FP7/20072013) (www.crescendo-fp7.eu) under grant agreement no. 234344. Authors are very thankful to engineers and researchers that helped to define and perform this work, particularly Praful Soneji and Richard Golder from Rolls-Royce, UK and Stéphane Grihon from Airbus, France.

References

1. Anonymous. *Demonstration Problems Manual: MSC Nastran 2012*. MacNeal-Schwendler Corporation, 2012.
2. D. Bettebghor, N. Bartoli, S. Grihon, J. Morlier, and M. Samuelides. Surrogate modeling approximation using a mixture of experts based on em joint estimation. *Structural and Multidisciplinary Optimization*, 43(2):243–259, 2011.
3. JB Cardoso and JS Arora. Design sensitivity analysis of nonlinear dynamic response of structural and mechanical systems. *Structural and Multidisciplinary Optimization*, 4(1):37–46, 1992.
4. K.S. Carney, C. Lawrence, and D.V. Carney. Aircraft engine blade-out dynamics. In *Seventh international LS-DYNA users conference. Livermore CA, USA: Livermore Software Technology Corporation*, pages 14–17, 2002.
5. S. Cho and KK Choi. Design sensitivity analysis and optimization of non-linear transient dynamics. part 1: sizing design. *International Journal for Numerical Methods in Engineering*, 48(3):351–373, 2000.
6. K.K. Choi and N.H. Kim. *Structural sensitivity analysis and optimization: nonlinear systems and applications*, volume 2. Springer, 2005.
7. A.I.J. Forrester and A.J. Keane. Recent advances in surrogate-based optimization. *Progress in Aerospace Sciences*, 45(1):50–79, 2009.
8. J. Friedman, T. Hastie, and R. Tibshirani. The elements of statistical learning, 2001.
9. S. Grihon. Pylon design optimisation. In *Forum 1, VIVACE project*, 2005.
10. R.T. Haftka and H.M. Adelman. Recent developments in structural sensitivity analysis. *Structural and Multidisciplinary Optimization*, 1(3):137–151, 1989.
11. M. Heidari, D.L. Carlson, S. Sinha, R. Sadeghi, C. Heydari, H. Bayoumi, and J. Son. An efficient multidisciplinary simulation of engine fan-blade out event using md nastran. *American Institute of Aeronautics and Astronautics*, 2008.
12. M.A. Heidari, D.L. Carlson, and T. Yantis. Rotordynamics analysis process. In *MSC Worldwide Aerospace Conference and Technology Showcase*, pages 1–16, 8-10 April, 2002.
13. CC Hsieh and JS Arora. Design sensitivity analysis and optimization of dynamic response. *Computer Methods in Applied Mechanics and Engineering*, 43(2):195–219, 1984.
14. J.B. Husband. *Developing an efficient FEM structural simulation of a fan blade off test in a turbofan jet engine*. PhD thesis, University of Saskatchewan, 2007.
15. R. Jain. Prediction of transient loads and perforation of engine casing during blade-off event of fan rotor assembly. In *Proceedings of the IMPLAST 2010 Conference, October 12-14 2010 Providence, Rhode Island USA*, 2010.
16. B.S. Kang, G.J. Park, and J.S. Arora. A review of optimization of structures subjected to transient loads. *Structural and Multidisciplinary Optimization*, 31(2):81–95, 2006.
17. M.C. Kennedy and A. O'Hagan. Predicting the output from a complex computer code when fast approximations are available. *Biometrika*, 87(1):1–13, 2000.
18. Y.I. Kim and G.J. Park. Nonlinear dynamic response structural optimization using equivalent static loads. *Computer Methods in Applied Mechanics and Engineering*, 199(9-12):660–676, 2010.
19. YI Kim, GJ Park, RM Kolonay, M. Blair, and RA Canfield. Nonlinear dynamic response structural optimization of a joined-wing using equivalent static loads. *Journal of aircraft*, 46(3):821–831, 2009.
20. S.B. Lattime, B.M. Steinetz, and NASA Glenn Research Center. *Turbine engine clearance control systems: Current practices and future directions*. National Aeronautics and Space Administration, Glenn Research Center, 2002.
21. C. Lawrence, K. Carney, and V. Gallardo. *A Study of Fan Stage/Casing Interaction Models*. National Aeronautics and Space Administration, Glenn Research Center, 2003.
22. C. Lawrence, K.S. Carney, V. Gallardo, and NASA Glenn Research Center. *Simulation of Aircraft Engine Blade-Out Structural Dynamics*. National Aeronautics and Space Administration, Glenn Research Center, 2001.
23. R.T. Marler and J.S. Arora. Survey of multi-objective optimization methods for engineering. *Structural and multidisciplinary optimization*, 26(6):369–395, 2004.
24. G. Michels, V. Genberg, and K. Doyle. Using the dresp3 to improve multidisciplinary optimization. *MSC Software*, pages 2004–30, 2004.

25. K. Miettinen. *Nonlinear multiobjective optimization*, volume 12. Springer, 1999.
26. M.C.Y. Niu. Airframe structural design: practical design information and data on aircraft structures. *Recherche*, 67:02, 1999.
27. G.J. Park. Technical overview of the equivalent static loads method for non-linear static response structural optimization. *Structural and Multidisciplinary Optimization*, 43(3):319–337, 2011.
28. SS Rao and TI Freiheit. A modified game theory approach to multiobjective optimization. *Journal of Mechanical Design*, 113:286, 1991.
29. T.L. Saaty. A scaling method for priorities in hierarchical structures. *Journal of mathematical psychology*, 15(3):234–281, 1977.
30. S.K. Sinha and S. Dorbala. Dynamic loads in the fan containment structure of a turbofan engine. *Journal of Aerospace Engineering*, 22:260, 2009.
31. D.J.J. Toal, N.W. Bressloff, A.J. Keane, and C.M.E. Holden. The development of a hybridized particle swarm for krigign hyperparameter tuning. *Engineering Optimization*, 43(6):675–699, 2011.
32. JJ Tsay and JS Arora. Nonlinear structural design sensitivity analysis for path dependent problems. part 1: General theory. *Computer Methods in Applied Mechanics and Engineering*, 81(2):183–208, 1990.
33. J.M. Vance. *Rotordynamics of turbomachinery*. Wiley-Interscience, 1988.
34. J.M. Vance, B. Murphy, and F. Zeidan. *Machinery vibration and rotordynamics*. Wiley Online Library, 2010.

A Preliminary modal analysis

In this short section, we simply describe the numerical results obtained for modal analysis of the whole structure. As outlined in Section 5 one may observe numerical resonance issues when the spinning speed of rotors approaches natural frequencies of the structure. We than ran a preliminary modal analysis to ensure that the rotor nominal spinning speed is not near any natural frequencies. As noted in the article, the nominal rotor speed of the rotor is 50 Hz and the windmill speed is 10 Hz. Both frequencies are not close to a natural eigenfrequencies of the assembly. For sake of completeness, we also depicted the shapes of the first natural modes of the assembly.

Modes	Hz (Hertz)
1	3.05
2	5.76
3	6.84
4	7.96
5	12.56
6	13.5
7	14.67
8	15.01
⋮	⋮
20	34.5
⋮	⋮
27	48.2
28	51.47

Table 1 Eigenfrequencies of the pylon-engine-nacelle assembly.

B Implementation details for FBO rotor dynamics simulation and optimization session

We briefly describe here the different solutions that we used to achieve our bi-objective optimization. The final assembled model was a MSC.Nastran FEM model. Based on our previous experience, we ran the optimization with MSC.Nastran solution SOL200. More precisely we used the different items:

- Classical SOL101 and SOL103 were used first to run and validate our final finite element model. SOL101 was used first to ensure that no major issue nor mistake was in the model. SOL103 was used to compute the first fundamental modes of the assembled structure and get the first fundamental frequencies to get rid off resonance issue while performing rotordynamics issue. SOL101 and SOL103 solutions were used for the material linear part of the model: engine and pylon assembly.
- We first ran Fan Blade Off event simulation based on Rolls-Royce, UK entries. To that end, we started with linear modeling and ran transient and direct dynamics analysis solutions from MSC: SOL109 and SOL112. When facing unreasonable output responses, we enriched our model and reaches a more realistic model by integrating nacelle and rotordynamics effects.
- Whenever the nacelle was added, we had to turn to nonlinear dynamics solution : SOL129. The same way, we used in this solution the rotordynamics Nastran cards: `RGYRO`, `ROTORG`, etc. As already noticed, simulation results were similar to responses that we would expect for such a simulation, however, for our design optimization, we needed to extract forces at pylon-to-wing and engine-to-pylon attachment. This could not be done in SOL129. We then had to use SOL400 for nonlinear dynamics simulation to retrieve Nastran `SPCFORCES` cards.
- To create our equivalent FBO static load cases, we used classical text processing languages such as shell scripts and awk. MATLAB has also been used to post-process results.
- Regarding SFC surrogate model, we could not directly use the webservice in SOL200. Indeed, such an integration seems hardly feasible[4] since a MATLAB executable is not suited to integration in the external response driver of SOL200. Such a technology is indeed easier with the source code. This is why we did use a surrogate model of the surrogate model, to get our known source code. To approximate the surrogate model of SFC, we used a different strategy than the one used by University of Southampton that was kriging models. We used a mixture of experts strategy, described in [2].
- Optimization was performed with SOL200. The SFC surrogate model was integrated using `DRESP3` card, a quite popular tool for multidisciplinary optimization, see for instance [24]. The Pareto front was then obtained by automating the process of changing the weighting factor in a scalar optimization through standard shell scripting.

[4] still possible though

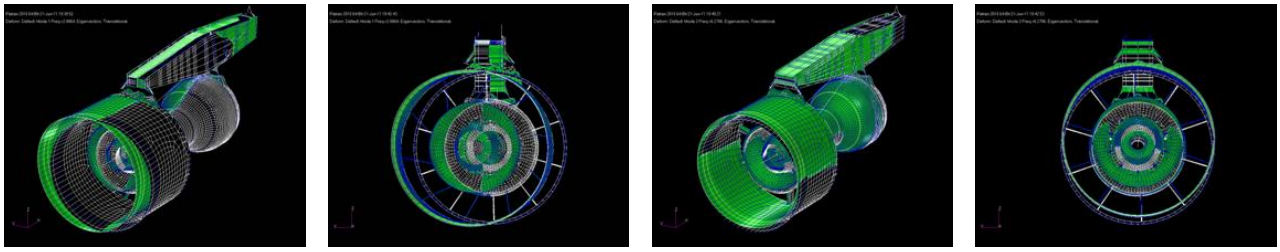

(a) (b) (c) (d)

Fig. 13 First two fundamental modes of the engine-pylon-nacelle assembly. Note that nacelle is not represented for clarity of shape modes. a) and b) First fundamental mode: $F = 3.05$ Hz, c) and d) second fundamental mode $F = 5.76$ Hz.

C Transient loads history in attachments

We can not give all the transient history for all attachments. However, for sake of comparison, for instance with [14], we present in this section the history of loads for pylon-to-wing attachments. As it can be observed in Fig. 14 when comparing with results in [14], forces are quite similar in terms of magnitude and pseudo-period.

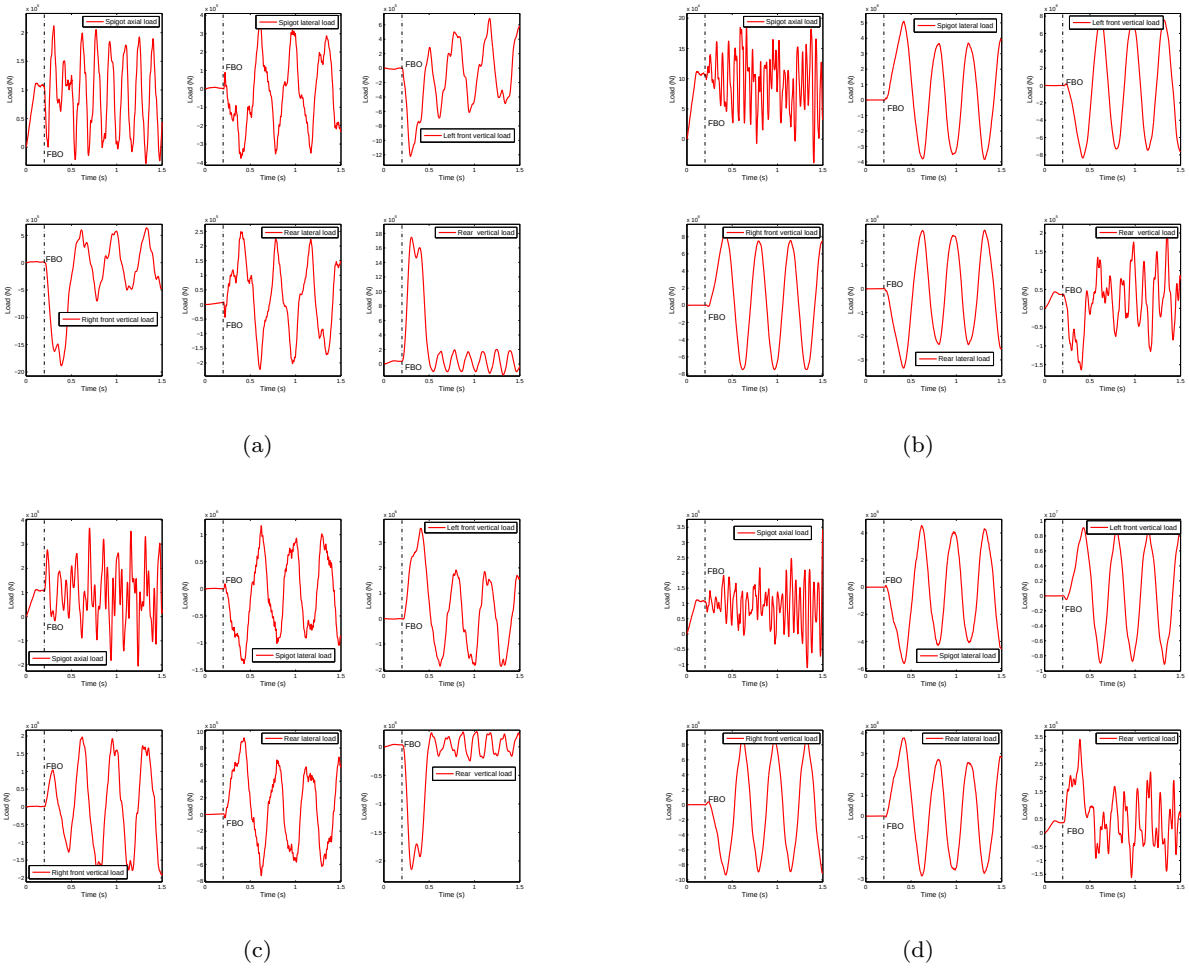

Fig. 14 Transient loads for FBO event at pylon-to-wing attachment a) Release angle 0°, b) Release angle 90°, c) Release angle 180°, d) Release angle 270°.